Journal of Thermal Analysis and Calorimetry (2019) 135:507–522
https://doi.org/10.1007/s10973-018-7074-5

Toward a modeling study of thermal conductivity of nanofluids using LSSVM strategy

Alireza Baghban[1] · Sajjad Habibzadeh[1,2] · Farzin Zokaee Ashtiani[2]

Received: 20 January 2018 / Accepted: 10 February 2018 / Published online: 21 February 2018

Abstract

In the present study, a comprehensive model based on least square support vector machine algorithm (LSSVM) was developed to estimate thermal conductivity of nanofluids. The model assessed the thermal conductivity of 29 different nanofluids. The representative nanofluids were composed of nine base fluids, including water, ethylene glycol, transformer oil, engine oil, R113, DI Water, monoethylene glycol, paraffin, and oil. Al_2O_3, TiO_2, CuO, ZnO, Al, and Cu nanoparticles were employed in the corresponding nanofluids. A collection of 1109 experimental samples from reliable sources was used. In addition, the present model can estimate the thermal conductivity of nanofluids as a function of temperature, diameter, nanoparticle volume fraction as well as the thermal conductivity of the nanoparticles and the base fluid. The proposed LSSVM structure was optimized by particle swarm optimization technique where the outcomes proved great accuracy of the model for estimating the thermal conductivity of nanofluids. Moreover, statistical observations showed superior predictive ability of LSSVM model than other previous available correlations. Namely, the average relative deviation percent of 2.46 and 3.10%, and *R*-squared values of 0.9954 and 0.9914 were resulted for training and testing stages of LSSVM model, respectively.

Keywords Nanofluid · Thermal conductivity · Least square support vector machine algorithm · Particle swarm optimization · Sensitivity analysis · Outlier analysis

Introduction

Extensive utilizations of heat transfer phenomena in industrial instruments underlie their great significance in the corresponding efficiency. Further, economic heat transfer processes are characterized by the required volume of such instruments, which is, in turn, related to their efficiency [1, 2]. Therefore, the required power consumption and thus processing cost decrease with an increase in the heat transfer efficiency of the working fluid passing through the heat transfer devices. Numerous investigations have been carried out in order to enhance the efficiency of heat transfer [3–5]. Increasing the effective surface area, utilization of vibration technique and application of microscale channels are such investigations that can improve the efficiency of heat transfer. As demonstrated in Fig. 1, one can observe remarkable attentions on nanofluid systems based on annually published articles. This figure was prepared based on publications recorded in Google Scholar, which are searched in January 2018 by three relevant topics such as "nanofluids", "nanofluids thermal conductivity", and "nanofluids viscosity" during various years. As can be seen, the main investigated subject regarding the nanofluid systems refers to the thermal conductivity (42%), followed by viscosity (58%). On the other hand, the thermal conductivity of the working fluid in the heat transfer systems is identified as an important factor as to improve the heat transfer efficiency. Owning to low thermal conductivity of traditional working heat transfer fluids, for example, water (H_2O), ethylene glycol (EG), and

Electronic supplementary material The online version of this article (https://doi.org/10.1007/s10973-018-7074-5) contains supplementary material, which is available to authorized users.

✉ Alireza Baghban
alireza_baghban@alumni.ut.ac.ir

✉ Sajjad Habibzadeh
sajjad.habibzadeh@aut.ac.ir

[1] Amirkabir University of Technology (Tehran Polytechnic), Mahshahr Campus, Mahshahr, Iran

[2] Chemical Engineering Department, Amirkabir University of Technology (Tehran Polytechnic), Tehran, Iran

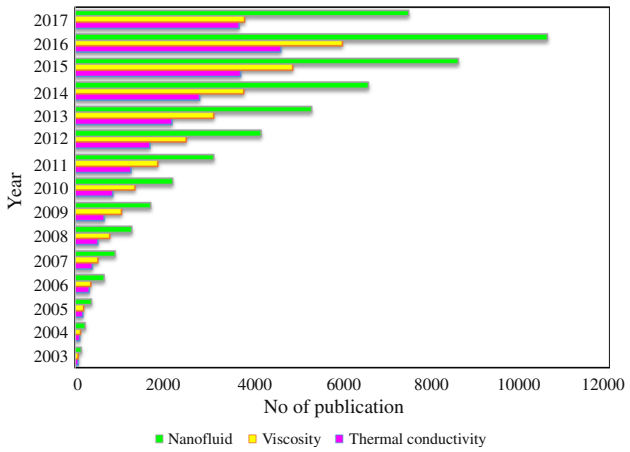

Fig. 1 Year-wise published research records on different areas of nanofluids from Google scholar (2003–2017)

different oils, their thermal conductivity can be increased through the addition of a few solid nanoparticles to such aforementioned fluids [6, 7]. These nanoparticles help to have a simple fluidized process, avoiding critical issues, such as the blockage of channels, precipitation of particles, and erosion due to their nano-sized structures. A new aspect of nanofluids was familiarized by Chol [8] considering the suspension of nanoparticles in a base fluid. In addition, a practical application of nanofluids in microchannels was also introduced [9]. Recently, numerous studies have been carried out in order to predict the nanofluids thermal conductivity using simple empirical correlations and some analytical solutions. A simple correlation was proposed by Maxwell [10] in 1904 for determining the nanofluid's effective thermal conductivity. This correlation can be employed in order to estimate the thermal conductivity in dilute suspensions containing microparticles; however, this correlation could not show an accurate estimation of the thermal conductivity of nanofluids high deviations between correlation and experimental results [11–14].

Several studies have reported the measured thermal conductivity of nanofluids together with the effective parameters. Such parameters found to be the volume fraction of nanoparticles and their size, the aggregation, morphology and the physicochemical properties of the solid particles, as well as temperature, and the nature of the base fluid. In addition, many efforts have been made to proposing theoretically a new mechanism for thermal conductivity enhancement. An investigation was carried out by Vatani et al. [15] to estimate effective thermal conductivity of nanofluids based on broad data gathering from recent articles. They compared the outcomes of their model with seven previous other correlations and concluded that all the models cannot be accurately applied for different nanofluids; nonetheless, these available correlations are quite popular in the estimation of nanofluid's thermal conductivity. As a result, highly accurate estimation of thermal conductivity of nanofluids is a stimulating subject which must be addressed. Moreover, measuring the thermal conductivity of nanofluids seems to be time-consuming and costly while limited effective parameters can be investigated during the experiments [16]. On the other hand, the proposed available models can also cover inadequate ranges of working conditions. Accordingly, developing an accurate model to indicate the relationships between relevant parameters determining the thermal conductivity of nanofluids was found to be a serious issue. An investigation was carried out by Baghban et al. to estimate heat transfer coefficient of the nanofluids containing the silica nanoparticles as a function of Reynolds number, Prandtl number, and mass fraction nanofluid by the adaptive neuro-fuzzy inference system (ANFIS), artificial neural network (ANN), support vector machine (SVM), least square support vector machine (LSSVM), genetic programming (GP), principal component analysis (PCA), and committee machine intelligent system (CMIS) [17].

To address such issue employing artificial intelligence, such as the artificial neural networks (ANNs), fuzzy inference systems, and support vector machines, which typically result in precise outcomes, has been recommended by numerous studies in several fields [18–23]. ANN is known as a promising technique to find optimal solutions for complicated problems leading to a considerably time- and/or cost-saving procedure. Thanks to the rapid process of the ANN, it has broadly applications in numerous studies in order to estimate the thermophysical properties of nanofluids, i.e., thermal conductivity, density, and viscosity [24–27]. An artificial neural network model has been proposed by Hojjat et al. [28] to estimate the thermal conductivity of non-Newtonian nanofluids. The inputs of their model were based on the operating temperature, the concentration and thermal conductivity of nanoparticles. In addition, another model developed by Papari et al. [29] was based on a diffusion neural network approach. Such model was employed to predict the thermal conductivity of certain nanofluids containing multi-walled carbon nanotubes. The nanofluids were synthesized in four base fluid including oil, decene, distilled water, and ethylene glycol. A couple of structures of ANN model were also applied by Longo et al. [30] in order to predict the thermal conductivity of Al_2O_3 and TiO_2 nanopowders in water as the base fluid. The model was developed as a function of temperature, volume fraction, thermal conductivity, and the average size of nanoparticle. Hemmati Esfe et al. [31] modeled the thermal conductivity of Al_2O_3–Water nanofluid at different temperatures and solid volume fractions using ANN method. Recently, another

embranchment of artificial intelligence called least square support vector machine has been employed by numerous scholars in such fields [19–21]. However, this technique has been rarely utilized in order to estimate the physical properties of nanofluids [32]. It would be worth mentioning that all previously proposed models can only be applied for limited nanofluids with poor accuracy to estimate thermal conductivity. Hence, the present work aims to present a more wide-ranging model for estimating the thermal conductivity of nanofluids.

Available correlations

Several operative medium models have been employed to predict the effective thermal conductivity of nanofluids. The correlation-based models, such as Maxwell correlation [33], Hamilton and Crosser correlation [34], and Bruggeman correlation [35] could predict the effective thermal conductivity of nanofluid as a function of volume fraction, the thermal conductivity of particle, and thermal conductivity of base fluid. Apart from these conventional correlation-based approaches, newly proposed strategies are also explained here. The effect of a nanolayer around a particle was considered by new approaches, such as Yu–Choi's [36], Leong's et al. [37], Xie et al.'s [38], and Sohrabi's models [39]. It is worth to mention that Sohrabi's [39], Koo and Kleinstreuer's [40], and Xu et al.'s models [41] considered the effect of convective heat transfer caused by Brownian motion in their models. Moreover, an investigation was carried out by Evans et al. [42] in order to show the dependence of thermal conductivity of nanofluids on clustering and interfacial thermal resistance. The following literature surveys encompass extensive conducted studies by researchers to predict thermal conductivity of nanofluids.

Maxwell correlation

This correlation (Eq. 1) is considered as the preliminary developed correlation which can predict the effective thermal conductivity of nanofluids [33]. Accurate outcomes of this model are resulted for low volume fractions of spherical particles.

$$K_{\text{eff}} = \frac{K_{\text{p}} + 2K_{\text{f}} + 2\phi\left(K_{\text{p}} - K_{\text{f}}\right)}{K_{\text{p}} + 2K_{\text{f}} - \phi\left(K_{\text{p}} - K_{\text{f}}\right)} K_{\text{f}} \tag{1}$$

Here k_{eff}, k_{f}, and k_{p} refer to the effective thermal conductivity of nanofluid, the thermal conductivity of the base fluid, and thermal conductivity of particle, respectively. ϕ stands for the volume fraction of the particle.

Hamilton and Crosser correlation (H–C model)

The main advantage of H–C model compared with Maxwell model is that the H–C model considered the effect of the particle shapes in their formulation. This model is formulated as below [34]:

$$K_{\text{eff}} = \frac{K_{\text{p}} + (n-1)K_{\text{f}} - (n-1)\phi\left(K_{\text{p}} - K_{\text{f}}\right)}{K_{\text{p}} + (n-1)K_{\text{f}} - \phi\left(K_{\text{p}} - K_{\text{f}}\right)} K_{\text{f}}, \quad n = \frac{3}{\psi} \tag{2}$$

In the above correlation, the term n refers to the empirical shape factor and ψ stands for the sphericity, which is the ratio of the surface area of a sphere with unit volume to the surface area of the particle. In the case of $n = 3$, both H–C and Maxwell correlations are identical.

Bruggeman correlation

For spherical particles, the Bruggeman model [35] has more satisfactory prediction compared to the Maxwell model. This model uses another averaging technique with no restrictions on the concentration of inclusions. This model is formulated as follows:

$$K_{\text{eff}} = \left\{ \frac{1}{4}\left[(3\phi - 1)\frac{K_{\text{p}}}{K_{\text{f}}} + (2 - 3\phi) \right] + \frac{1}{4}\sqrt{\left[(3\phi-1)^2 \left(\frac{K_{\text{p}}}{K_{\text{f}}}\right)^2 + (2-3\phi)^2 + 2\left(2 + 9\phi - 9\phi^2\right)\left(\frac{K_{\text{p}}}{K_{\text{f}}}\right) \right]} \right\} K_{\text{f}} \tag{3}$$

All above available correlations had satisfactory accuracy for the large size of particles (micro- and millimeter), but their approximation for nano-size particles shows significant deviations.

The Yu and Choi model

A proper investigation was carried out by Yu and Choi [36] to show the effect of a nanolayer around a particle in nanofluids for calculating the corresponding thermal conductivity. Moreover, they assumed a quite low particle volume concentration in the base fluid. Accordingly, the equivalent thermal conductivity of the equivalent particles k_{pe} can be expressed as [43]:

$$K_{\text{pe}} = \frac{\left[2(1-\sigma) + (1+\beta)^3(1+2\sigma)\right]\sigma}{-(1-\sigma) + (1+\beta)^3(1+2\sigma)} K_{\text{p}} \tag{4}$$

where $\beta = \frac{h}{a}$ in which h refers to the thickness of the nanolayer and a stands for the radius of particle. In addition, the definition of σ is $\sigma = \frac{k_{\text{lr}}}{K_{\text{p}}}$ in which k_{lr} denotes the nanolayer thermal conductivity and k_{p} is the thermal conductivity of particle. Yu and Choi modified the above

correlation with the following formula by combining with the Maxwell model, which is shown as follows:

$$K_{pe} = \frac{K_{pe} + 2K_f + 2(K_e - K_f)(1+\beta)^3\phi}{K_{pe} + 2K_f - (K_e - K_f)(1+\beta)^3\phi} K_f \quad (5)$$

It should be mentioned that there is a limiting case as $\sigma = 1$ in the Yu–Choi model. Accordingly, this model can help us to have forward computations for thermal conductivity of nanofluids in the presence of a nanolayer.

Leong et al.'s correlation

The proposed formula by Leong et al. [37] to determine the effective thermal conductivity of nanofluids was developed via solving the energy equation in spherical coordinates at steady-state condition which is presented as below:

$$k_{eff} = \frac{(k_p - k_{lr})\phi k_{lr}\left[2\gamma_1^3 - \gamma_2^3 + 1\right] + (k_p - 2k_{lr})\gamma_1^3\left[\phi\gamma_2^3(k_{lr} - k_f) + k_f\right]}{\gamma_1^3(k_p + 2k_{lr}) - (k_p - k_{lr})\phi\left[\gamma_1^3 + \gamma_2^3 - 1\right]} \quad (6)$$

In above expression, $\gamma_1 = 1 + \frac{h}{2a}$ and $\gamma_2 = 1 + \frac{h}{a}$ and also k_{lr} refers to the thermal conductivity of the interfacial nanolayer. As can be concluded from the Leong et al. model, the effective thermal conductivity is related to the particle' radius (a), interfacial nanolayer thickness (h), volume fraction (ϕ), and the thermal conductivity of the particle (k_p) and the base fluid (k_f). The Maxwell model can be obtained from this formula when $k_{lr} = k_f$ and $h = 0$. Leong et al.'s model used the general solution for the base liquid temperature field (T_f). By this modification, the model can be reduced to the Maxwell model by either setting $h = 0$ or $k_{lr} = k_f$.

Xie et al.'s model

Another investigation was carried out by Xie et al. [38] to propose a model for thermal conductivity of nanofluids in the presence of a nanolayer with spherical shell and thickness (h) around the particle. The following formula indicates their model as:

$$k_{eff} = k_f + 3\theta\phi_T k_f + \frac{3\theta^2\phi_T^2}{1 - \theta\phi_T} k_f \quad (7)$$

Here, term θ can be obtained by:

$$\theta = \frac{\left(\frac{k_{lr} - k_f}{k_{lr} + 2k_f}\right)\left[\left(1 + \frac{h}{a}\right)^3 - \frac{\left(\frac{k_p - k_f}{k_p + 2k_f}\right)}{\left(\frac{k_f - k_{lr}}{k_f + 2k_{lr}}\right)}\right]}{\left(1 + \frac{h}{a}\right)^3 + 2\left(\frac{k_{lr} - k_f}{k_{lr} + 2k_f}\right)\left(\frac{k_p - k_{lr}}{k_p + 2k_{lr}}\right)} \quad (8)$$

ϕ_T which refers to the total volume fraction of nanoparticles and nanolayers are defined as follows:

$$\phi_T = \phi\left(1 + \frac{h}{a}\right)^3 \quad (9)$$

The thermal conductivity of the nanolayer (k_{lr}) can be introduced as:

$$k_{lr} = \frac{k_f\left[\frac{k_p}{k_f}\left(1 + \frac{h}{a}\right) - 1\right]^2}{\left\{\left[\frac{k_p}{k_f}\left(1 + \frac{h}{a}\right) - 1\right] - \frac{h}{a}\right\}\ln\left\{1 + \left[\frac{k_p}{k_f}\left(1 + \frac{h}{a}\right) - 1\right]\right\} + \frac{h}{a}\left[\frac{k_p}{k_f}\left(1 + \frac{h}{a}\right) - 1\right]} \quad (10)$$

A similar model developed by Sohrabi et al. [39] showed the effect of the convective heat transfer caused by the Brownian motion. They considered linear and nonlinear profiles for the thermal conductivity of the nanolayer. As Xie et al., they did not directly use such profiles in their main equations and an average value of the nanolayer thermal conductivity was employed to determine the effective thermal conductivity of nanofluids.

Koo and Kleinstreuer's model

The model developed by Koo and Kleinstreuer [13] predicts the thermal conductivity of nanofluids as a function of k_{static} and $k_{Brownian}$. The former term (k_{static}) in the thermal conductivity is owing to the higher thermal conductivity of the nanoparticles, while the latter ($k_{Brownian}$) implies the effect of Brownian motion. The above-mentioned conventional Maxwell model is employed for determining static term, and Brownian motion effects are defined as expressed by the following formula.

$$k_{Brownian} = 5 \times 10^4 \beta\phi\rho_f C_{p,f}\sqrt{\frac{k_B T f}{\rho_p d_p}} \quad (11)$$

The density of particles and base fluid is shown by ρ_p and ρ_f, respectively; also T and $c_{p,f}$ refer to the operating temperature and specific heat capacity of the base fluid, respectively. k_B is the Boltzmann's constant, and d_p stands for the particle diameter. The empirical terms in formulation 11 (β and f) are obtained by accurate experimental measurements. In addition, Koo and Kleinstreuer [40] suggested a method for determining β, while f can be obtained based on the following expression.

$$f = (-134.63 + 1722.3\phi) + (0.4705 - 6.04\phi)T \quad (12)$$

Indeed, developing expressions for f and β are a problematic issue because of their complications. Hence, Xu et al. [41] suggested another model to address this problem.

Xu et al.'s model

Another strategy similar to Koo and Kleinstreuer model was proposed by Xu et al. [41]. The thermal conductivity

of nanofluids is composed of two terms of static and dynamic conductivity. The dynamic term in this model differs from the one in Koo and Kleinstreuer model [13]. They assumed that the distribution of the nanoparticle sizes is fractal, resulting in the following expression for the dynamic part of the thermal conductivity of nanofluids.

$$k_{\text{Dynamic}} = k_{\text{f}} C \frac{Nu \times d_{\text{f}}(2-D_{\text{f}})D_{\text{f}}\left[\left(\frac{d_{\text{p,max}}}{d_{\text{p,min}}}\right)^{1-D_{\text{f}}}-1\right]^2}{Pr(1-D_{\text{f}})^2\left(\frac{d_{\text{p,max}}}{d_{\text{p,min}}}\right)^{2-D_{\text{f}}}-1} \times \frac{1}{\bar{d}_{\text{p}}} \tag{13}$$

Here D_{f} is defined as:

$$D_{\text{f}} = 2 - \frac{\ln \phi}{\ln\left(\frac{d_{\text{p,mx}}}{d_{\text{p,min}}}\right)} \tag{14}$$

C, $\bar{d}_{\text{p}}$, d_{f}, $d_{\text{p,min}}$, and $d_{\text{p,max}}$ refer to empirical coefficient, average diameter, diameter of the liquid molecule, minimum and maximum particle diameters, respectively. In addition, Xu et al. employed Tomotika et al. [44] approach presented in the following equation to determine Nusselt number while assuming $\frac{d_{\text{p,max}}}{d_{\text{p,min}}} = 0.001$ is:

$$Nu = 2 + 0.5RePr + O\left(Re^2Pr^2\right) \tag{15}$$

The formulations of Reynolds and Prandtl number are expressed as:

$$Re = \frac{d_{\text{p}}u_{\text{p}}}{\vartheta_{\text{f}}} \tag{16}$$

$$Pr = \frac{\mu_{\text{f}}C_{\text{p,f}}}{k_{\text{f}}} \tag{17}$$

In above formulations, the velocity of particles is represented by u_{p}. μ_{f} and υ_{f} refer to the dynamic and kinematic viscosity of the base fluid, respectively. Moreover, the values of c for deionized water and ethylene glycerol (EG) were assumed by 85.0 and 280.0, respectively.

Evans et al.' model

Since clusters can be simply created by nanoparticles [45, 46], the fractal theory is typically applied to investigate such effect [47]. Evans et al. [42] believed that clustering can be as a consequence of rapid heat transfer along long distances. This is because of the conduction heat transfer rate through the solid particles is greater than that of liquid media. Hence, they studied the effect of clusters on thermal properties of nanofluids including the thermal conductivity and interfacial thermal resistance. Three models were utilized regularly to evaluate the effect of clusters including Bruggeman model, Nan et al. model [48], and Maxwell model. Accordingly, the following formula was obtained for the effective thermal conductivity of nanofluids.

$$k_{\text{eff}} = \frac{(k_{\text{cl}} + 2k_{\text{f}}) + 2\phi_{\text{cl}}(k_{\text{cl}} - k_{\text{f}})}{(k_{\text{cl}} + 2k_{\text{f}}) - \phi_{\text{cl}}(k_{\text{cl}} - k_{\text{f}})}k_{\text{f}} \tag{18}$$

The volume fraction and thermal conductivity of the clusters are represented by ϕ_{cl} and k_{cl}, respectively. They proved that size of a cluster increases with a rise of the effective thermal conductivity.

It should be noted that in all above-mentioned existing models, various physical mechanisms were used to determine the thermal conductivity enhancement of the nanofluids.

Theory of least square support vector machine (LSSVM)

Although ANN-based models result in promising outcomes, they are not reproducible. This is because of changing the optimization bases and unsystematic initialization of this type of models. The support vector machine (SVM) supersedes ANN-based models by applying a range of inputs from nonlinear functions to multi-dimensional mappings. Input and output spaces are connected by linear decision surface. The SVM-based models need fewer adjustable parameters compared to ANN-based models. In addition, SV-based models must not set the number of hidden layers and corresponding neurons for these models, leading to more accurate generalization [49, 50].

Least square support vector machine (LSSVM), developed by Suykens and Vandewalle [49] in 1999, showed to be simpler than SVM. Some linear equations with support vectors were used to eliminate the quadratic programming problems, to reduce sophistications of optimization. In LSSVM models, the regression error is estimated by the difference between calculated values by LSSVM and the experimental values, whereas in SVM method, regression error is computationally optimized. In LSSVM, the optimization process is done as [51, 52]:

$$L_{\text{LSSVM}} = \frac{1}{2}w^{\text{T}}w + \mu\sum_{i=1}^{n} e_{\text{i}}^2 \tag{19}$$

It is used in the equation below:

$$y_{\text{i}} = w^{\text{T}}g(x_{\text{i}}) + b + e_{\text{i}}, \quad i = 1, 2, 3, \ldots, n \tag{20}$$

where w is the weight vector, T is transposed matrix, μ shows a relation of single and total regression weight errors, e_{i} is the regression error dependent on entire data, $g(x)$ is a function of the mapping, and b is the bias term. W (regression weight coefficient) will be defined by applying Lagrangian multiplier (α_{i}) and an input vector (x_{i}) as:

$$w = \sum_{i=1}^{n} \alpha_i x_i \text{ in which } \alpha_i = 2\mu e_i \tag{21}$$

The equation above will be modified by considering a linear relationship between dependent and independent parameters as:

$$y = \sum_{i=1}^{n} \alpha_i x_i^T x + b \tag{22}$$

Then, Lagrange multiplier (α_i) will be obtained as:

$$\alpha_i = \frac{y_i - b}{x_i^T x + (2\mu)^{-1}} \tag{23}$$

The kernel function is combined with Eq. (23) as to modify it and make it usable for nonlinear constraints, so we would have:

$$y = \sum_{i=1}^{n} \alpha_i k(x_i, x) + b \tag{24}$$

where Kernel function [$k(x_i, x)$] is defined as:

$$k(x_i, x) = g(x_i) \cdot g(x)^T \tag{25}$$

The most common type of Kernels used in performing the LSSVM method is Gaussian radial basis function. Kernels (RBF kernels) and their samples are as follows:

$$k(x_i, x) = \exp\left(\frac{x_i - x^2}{\sigma^2}\right) \tag{26}$$

In which σ^2 is squared bandwidth and needs to be optimized by an optimization algorithm during the training process.

Results and discussion

Data preparation

Consistency and accuracy of the proposed models above highly depend on applied experimental data, which should be accessible and precise in order to implement the model [19, 21]. A comprehensive model was developed in the current study through using 1109 experimental data points for estimating dimensionless thermal conductivity of 29 different nanofluids at different particle diameter size, temperature, and volume fraction [11, 53–78]. It is worth mentioning that this model is applied for spherical nanoparticles. The name of studied nanofluids, ranges of temperature, particle diameters, and volume fractions together with their references are presented in Table 1. Moreover, the thermal conductivity of particles and base fluids is also summarized in Table 2. The next stage after data preparation and recognition is to select the input and output variables of the LSSVM model. The input variables of suggested LSSVM model were the temperature (K), particle diameter (nm), volume fraction (v), the thermal conductivity of nanoparticle (W m^{-1} K^{-1}), and thermal conductivity of the base fluid (W m^{-1} K^{-1}). On the other hand, the thermal conductivity of nanofluid was considered as the outcome of the model. Scheme of input and output variables of the proposed model is represented in Fig. 2. In order to train and evaluate the model, all gathered data points were divided into two subcategories, namely the test and train group. A quarter of data points was chosen as testing data, and the remained 75% was employed to train the LSSVM approach.

Model development and evaluation

Radial basis function (RBF) kernel renders high-speed computations owing to the fewer tuning terms as compared to others; such function was chosen as an operative and applicable kernel function in line with other studies. As already discussed, employing the proposed model which uses LSSVM approach with RBF kernel function deals with a significant problem, i.e., finding model tuning parameters of γ and σ^2 (where γ refers to the regularization term and σ^2 identifies the kernel sample variance). Such parameters play a remarkable role in order to achieve a satisfactory LSSVM model with high capability of approximations and globalizations.

The present research uses the particle swarm optimization (PSO) technique for determining optimal values of aforementioned tuning parameters. The objective of this optimization algorithm is to reach a less value of mean absolute relative error (MARE) of testing samples as a cost function. The optimization process was continued several epochs as efforts to obtain a possible global optimum based on the defined fitness function. Figure 3 illustrates a diagram of PSO–LSSVM model applied in the present work. Moreover, specifications of the proposed model are presented in Table 3.

A comparison between estimated and experimental thermal conductivity of nanofluid at three stages of training, testing, and total dataset for the LSSVM model is illustrated in Fig. 4. As is clearly seen in this figure, the

Table 1 Diameter, temperature, and volume fraction ranges of experimental data points

Systems	d_p/nm	T/K	Φ/%	No. of data points	References
Al–water	25–80	293–333	0.02–5	65	[53–57]
Al–TO					
Al–EG					
Al–EO					
Cu–water	80	293–323	0.1–3	75	[11, 55, 58]
Cu–EG	80	293–323	0.1–3		
Cu–oil	20	303–483	0.01–2.2		
Al_2O_3–water	11–150	273–353	0.015–9	351	[11, 56–58, 60, 63, 64]
Al_2O_3–EG	11–150			69	[57, 58, 65]
CuO–TO	31	293–324	0.01–14	16	[56]
CuO–water	18–33			138	[56, 60, 63, 64, 66–69]
CuO–EG	12–35			17	[56]
CuO–EMG	25			6	[64, 68]
CuO–MEG	30–40			8	[69]
CuO–paraffin	30–40			9	[69]
Al_2O_3–DI water	11–150	294–344	1–4	20	[11, 59]
TiO_2–EG	10–70	298	1–5	17	[57, 65]
TiO_2–DI water	10–70	298	1–3	9	[65]
TiO_2–water	18–76	283–352	0.005–11.22	51	[56, 67, 70]
ZnO–EG	30–70	283–343	1–6.2	309	[65, 71]
ZnO–DI water	10–60				
SiO_2–oil	15	296–380	1.2–7	25	[79]
SiO_2–water	10–12	298–353	0.015–5	24	[56, 72]
SiO_2–EG	12	298	0.05–0.4	4	[56]
MWCNT–water	9.2–15	293–313	0.005–0.8	17	[62, 73, 74]
MWCNT–EG	20		0.25–1	4	[62, 75]
MWCNT–Oil	25		0.25–1	5	[62, 76, 77]
MWCNT–R113	15–80		0.195–1	10	[62, 76]
Ag–Water	60–63	323–363	0.3–1.2	134	[61, 78]

estimated and actual thermal conductivities of nanofluid cover each other properly. Furthermore, the approximations by the proposed LSSVM model were assessed by applying various approaches such as the statistical and graphical confirmations. The cross-scheme of the suggested model which is created through scheming estimated against experimental data points of nanofluid' thermal conductivity is illustrated in Fig. 5. An excellent agreement between estimated and experimental nanofluid thermal conductivity values at different stages (i.e., train, test, and total's) is observed in this figure.

Figure 6 represents the percentage of absolute errors between the estimated thermal conductivity of nanofluid and experimental values. As can be seen, the vertical axis refers to the absolute error percent and the horizontal axes are assigned to the experimental thermal conductivity of nanofluid. Results from this figure indicate that the resulting errors by the LSSVM model range mostly between 5 and − 5%, confirming the promising performance ability of the proposed model. Apart from these graphical evaluations, a few popular statistical techniques which are expressed base on the following equations were applied. This can help to validate the superior application of our proposed model.

$$R^2 = 1 - \frac{\sum_{i=1}^{N}\left(y_{\mathrm{Pred}}(i) - y_{\mathrm{Exp}}(i)\right)^2}{\sum_{i=1}^{N}\left(y_{\mathrm{Pred}}(i) - \bar{y}_{\mathrm{Exp}}\right)^2} \tag{27}$$

$$\%\mathrm{AARD} = \frac{100}{N}\sum_{i=1}^{N}\frac{\left(y_{\mathrm{Pred}}(i) - y_{\mathrm{Exp}}(i)\right)}{y_{\mathrm{Exp}}(i)} \tag{28}$$

$$\mathrm{RMSE} = \left(\frac{\sum_{i=1}^{N}\left(y_{\mathrm{Pred}}(i) - y_{\mathrm{Exp}}(i)\right)^2}{N}\right)^{0.5} \tag{29}$$

$$\mathrm{STD} = \sum_{i=1}^{N}\left(\frac{\left(y_{\mathrm{Pred}}(i) - \bar{y}_{\mathrm{Exp}}(i)\right)^2}{N}\right)^{0.5} \tag{30}$$

Table 2 Thermal conductivity of nanoparticle and base fluid

Nanofluid	Thermal conductivity of particle/ W m^{-1} K^{-1}	Thermal conductivity of base fluid/ W m^{-1} K^{-1}
Al–Water	204	0.62
Al–TO	204	0.11
Al–EG	204	0.25
Al–EO	204	0.15
Cu–water	383	0.62
Cu–EG	383	0.25
Cu–oil	383	0.11
Al_2O_3–water	27	0.62
Al_2O_3–EG	27	0.25
CuO–TO	20	0.11
CuO–water	20	0.62
CuO–EG	20	0.25
CuO–EMG	20	0.27
CuO–MEG	20	0.27
CuO–paraffin	20	0.21
Al_2O_3–DI water	27	0.61
TiO_2–EG	8	0.25
TiO_2–DI water	8	0.61
TiO_2–water	8	0.62
ZnO–EG	29	0.25
ZnO–DI water	29	0.61
SiO_2–oil	1	0.12
SiO_2–water	1	0.62
SiO_2–EG	1	0.25
MWCNT–water	1800	0.62
MWCNT–EG	1800	0.25
MWCNT–oil	1800	0.25
MWCNT–R113	1800	0.07
Ag–water	420	0.62

The corresponding statistical analyses of the LSSVM model at three stages of train, test and total data points are summarized in Table 4. It is found that the LSSVM model results in high values of R-squared and low values of AARD, RMSE, and STD. These analyses strongly justify the applicability and consistency of the proposed model in order to estimate the thermal conductivity of nanofluids.

Several comparisons were carried out between the outcomes of the proposed LSSVM model and other previous correlations. Figure 7 shows the predicted dimensionless thermal conductivities of Al_2O_3–water nanofluid with particle diameter and temperature of 38.4 nm and 324 K, respectively, resulted from the models by Chon et al. [11], Murshed et al. [36], Nan et al. [38], Yu and Choi [48], Xie et al. [59], and Mintsa et al. [60] together with the ones from the proposed LSSVM model. The dimensionless thermal conductivity increases with an increase in the nanoparticle volume fraction. As can be seen, there is a great agreement between the LSSVM outcomes compared with other correlations. These correlations are simple and cannot be applied in different range of conditions. In addition, the dimensionless thermal conductivity of Ag–water nanofluid with a particle diameter of 63 nm at 343 K is obtained from the proposed model in this work, and correlations such as the Hamilton and Crosser [34], Timofeeva et al. [61], Wasp et al. [79], and Godson et al. [80] are compared in Fig. 8. Among these four correlations, after our LSSVM model, Godson et al. have satisfactory performance in order to apply in Ag–water system. This comparison clearly indicates an accurate prediction of the results from the present model proposed in this study with the corresponding experimental dimensionless thermal conductivities. Figure 9 shows the dimensionless thermal conductivity of carbon nanotube–water nanofluid predicted by Thang et al.'s correlation [62] as well as our proposed model at three different temperatures for $d_p = 9$ nm. In addition, another comparison of this correlation with LSSVM model for carbon nanotube–water nanofluid for different particle sizes at 296.15 K is indicated in Fig. 10. As can be seen for carbon nanotube–water nanofluid system, Thang et al.'s correlation cannot predict accurately the dimensionless thermal conductivity. Moreover, Fig. 11 shows the outcomes of the proposed LSSVM model and four other correlations developed by Patel et al. [81], Azmi et al. [82], and Vajjha and Das [83] for predicting the dimensionless thermal conductivity of CuO–water nanofluid with $d_p = 24$ nm and $T = 298.15$ K. Patel et al. have better accuracy than other two correlations for estimating dimensionless thermal conductivity in CuO–water system. In addition, the dimensionless thermal conductivity of TiO_2–EG nanofluid at 298.15 K resulted from Jang et al. correlation [84] and the proposed LSSVM model at different nanoparticle sizes and volume fractions is illustrated in Fig. 12. As can be found by all above comparisons, the LSSVM model proposed in this work shows an invaluable predictive ability to determine the dimensionless thermal conductivity of nanofluids.

Outlier detection and sensitivity analysis

It has been found that the data points used in the modeling study can highly influence the predictive performance of the resultant model [85]. Owning to different measurement errors of experimental databases in the literature, analysis

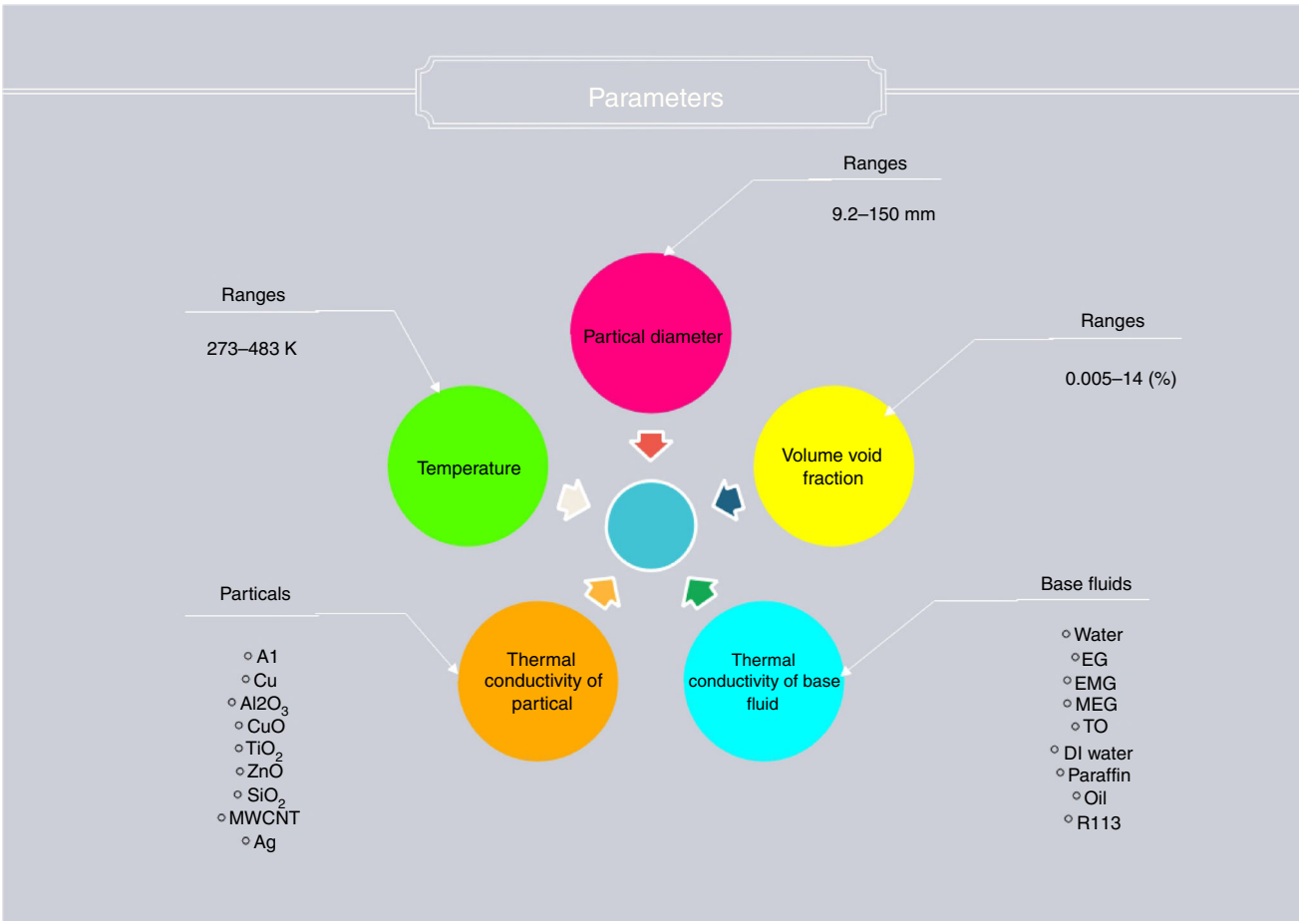

Fig. 2 Parameters used for implementation of the model

of outlier for applied data points can lead to erroneous measured data points. In order to carry out the outlier analysis, the leverage mathematical approach is usually used to calculate the residual values and Hat matrix of input data points as expressed below [86].

$$H = X\left(X^{\mathrm{T}}X\right)^{-1}X^{\mathrm{T}} \tag{31}$$

In the above equation, X stands for $m \times n$ matrix in which the terms m and n refer to the number of experimental measurements and parameters of our model, respectively. The main diagonal of Hat matrix can provide the Hat values. Consequently, a graphical illustration by William's plot indicates the valid and suspected data points. These results are shown in Fig. 13 to detect outliers. A warning leverage value (H^*) in this figure was calculated by:

$$H^* = 3(n+1)/m \tag{32}$$

Furthermore, the leverage boundary has been indicated by the green line and those data points which have higher Hat values (H) than this warning value H^* are introduced as outliers. Two other red lines presented in this figure are also referred to the standardized residuals boundaries with the values ranging $+3$ and -3. Accordingly, the valid data points are also situated within these boundaries.

Sensitivity analysis is a popular statistical technique to show the relationship between inputs and output. The effect of inputs on output term is determined by the relevancy factor (r). We can find the most effective variables on thermal conductivity of nanofluids for the present case. The relevancy factor is varied between -1 and $+1$. The higher value of this term is assigned to a specific input variable, indicating the more influence of this input variable on the corresponding output. The positive value is due to an increasing effect, and its negative value shows a

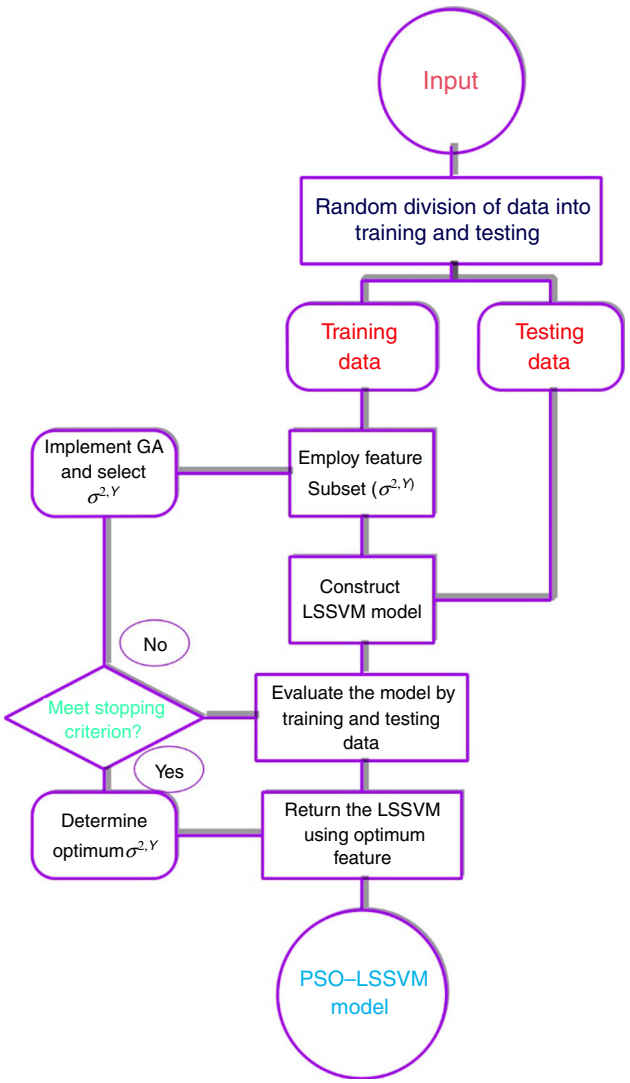

Fig. 3 Schematic diagram of proposed PSO–LSSVM model

Table 3 Details of trained LSSVM model

Type	Value/comment
No. of training data	961
No. of testing data	320
Kernel Function	RBF
γ	10,626.6529
σ^2	0.4326
Optimization method	PSO
Pop. size	110
Maximum iterations	1500
C_1	1
C_2	2

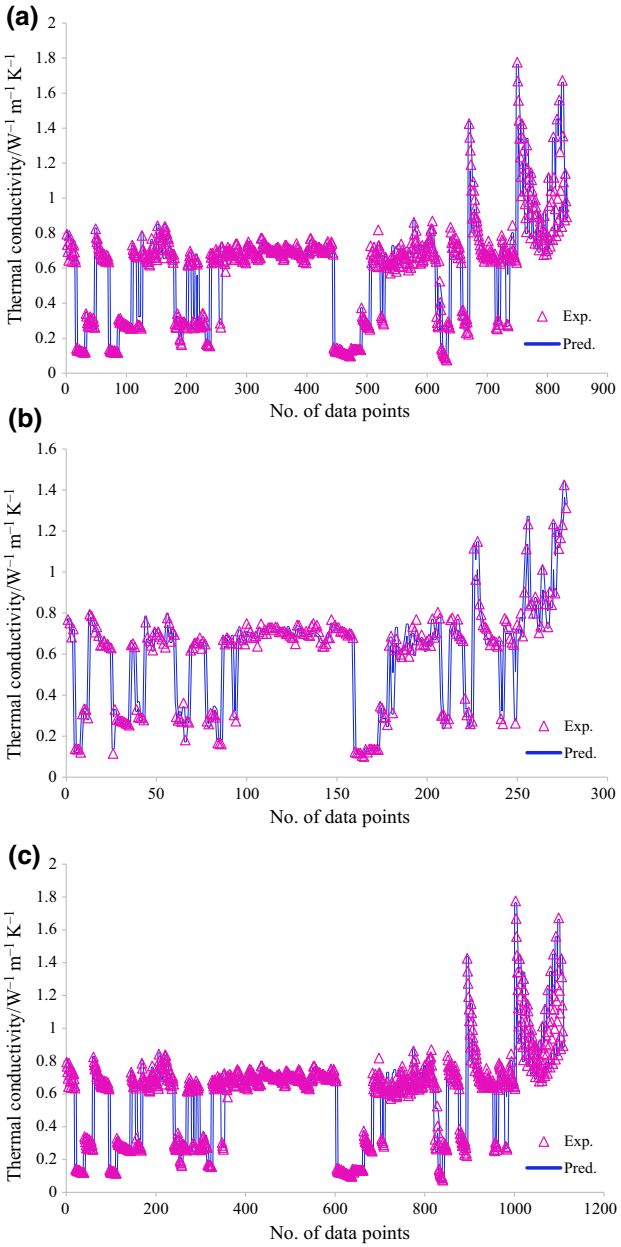

Fig. 4 Experimental versus estimated thermal conductivities for: **a** training data, **b** testing data, **c** total data

decreasing effect. A mathematical formulation of relevancy factor is defined as follows [87]:

$$r = \frac{\sum_{i=1}^{n}\left(X_{k,i} - \bar{X}_k\right)\left(Y_i - \bar{Y}\right)}{\sqrt{\sum_{i=1}^{n}\left(X_{k,i} - \bar{X}_k\right)^2 \sum_{i=1}^{n}\left(Y_i - \bar{Y}\right)^2}} \tag{33}$$

where $X_{k,i}$, $\bar{X}_k$, Y_i, and $\bar{Y}$ refer to the "i"th input value, the average value of the kth input, the "i"th output value, and the average value of output, respectively. Hence, as demonstrated in Fig. 14, the values of nanofluid

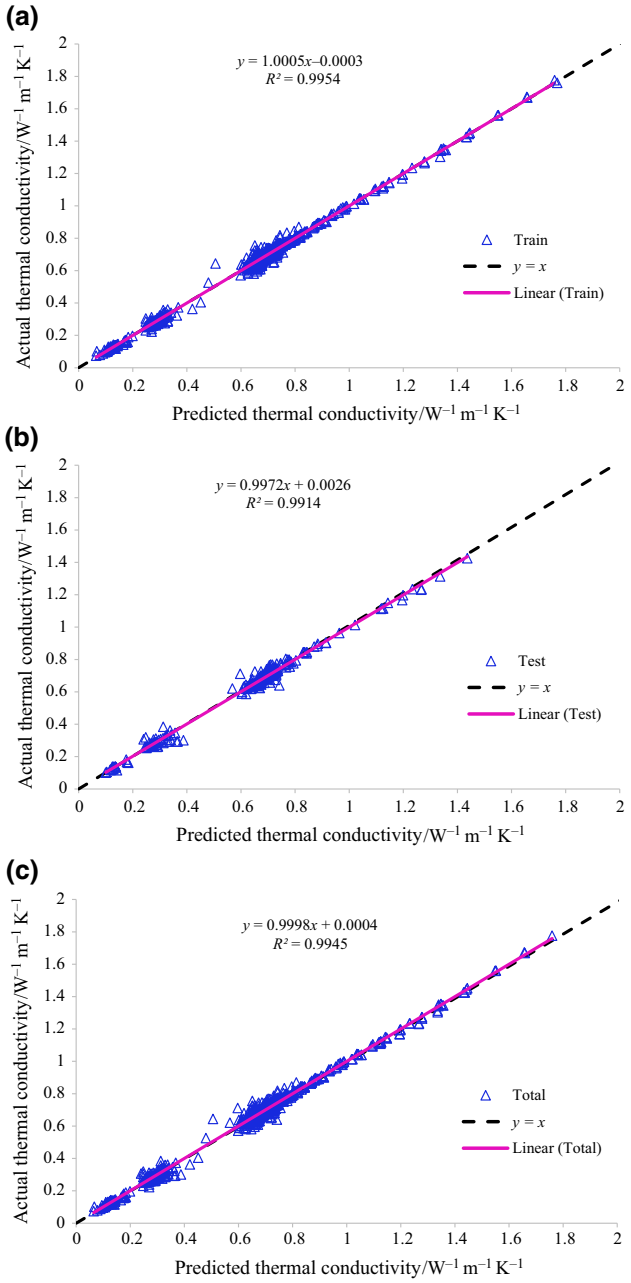

Fig. 5 Regression plots between experimental and estimated thermal conductivities for: **a** training data, **b** testing data, **c** total data

dimensionless thermal conductivity show a direct relationship between temperature, the thermal conductivity of base fluid, and volume fraction. Thermal conductivity of base fluid is the most effective parameter, and the particle diameter has the lowest effect on thermal conductivity of nanofluid. As can be seen, a number of sixty data points were detected as outliers.

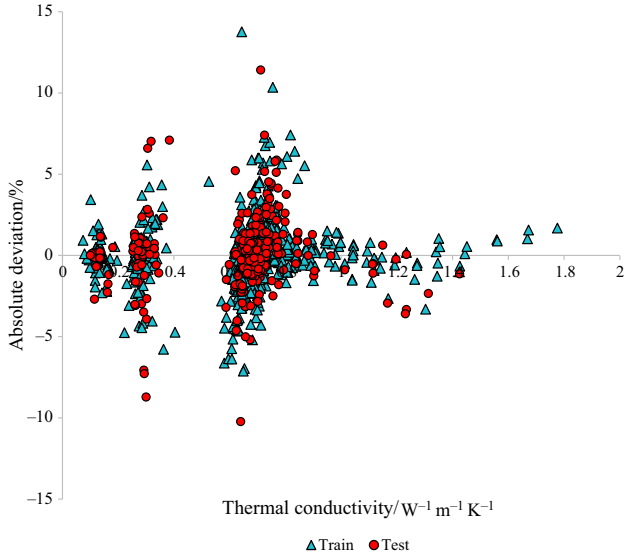

Fig. 6 Absolute deviation of the proposed LSSVM model

Table 4 Statistical analyses obtained from the LSSVM model

Analysis	Total	Training	Testing
R^2	0.994499	0.99535	0.991371
AARD/%	2.621034	2.462123	3.09834
MSE	0.0004	0.000354	0.000536
RMSE	0.019991	0.01882	0.023155
STD	0.015218	0.014345	0.017371

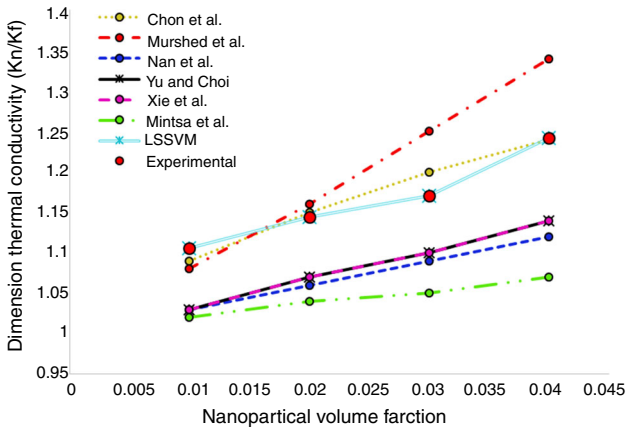

Fig. 7 Comparison of LSSVM model with different models to estimate dimensionless thermal conductivity of Al_2O_3–water nanofluid

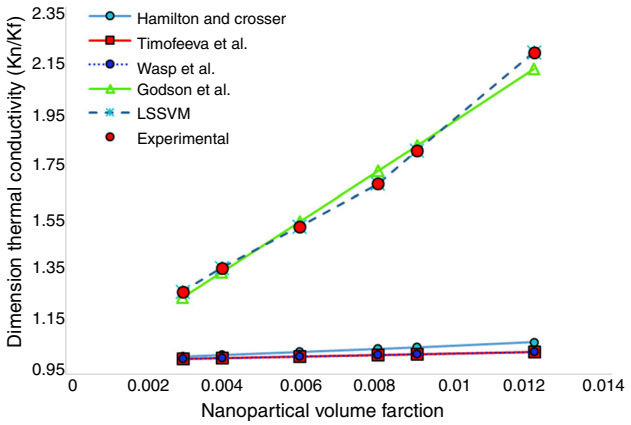

Fig. 8 Comparison of LSSVM model with different models to estimate dimensionless thermal conductivity of Ag–water nanofluid

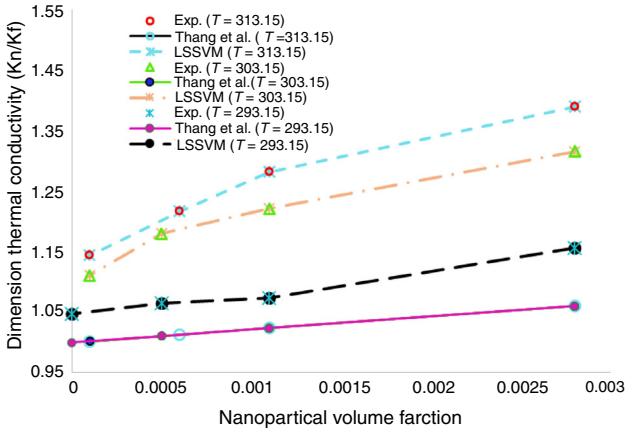

Fig. 9 Comparison of LSSVM model with Thang et al. model to estimate dimensionless thermal conductivity of CNT–water nanofluid at different temperatures

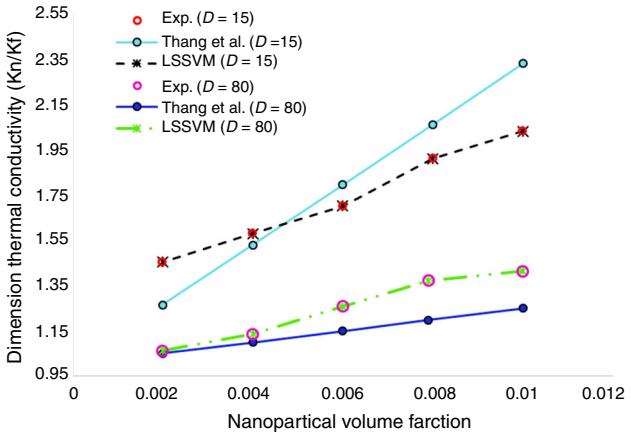

Fig. 10 Comparison of LSSVM model with Thang et al. model to estimate dimensionless thermal conductivity of CNT–water nanofluid for different particle sizes

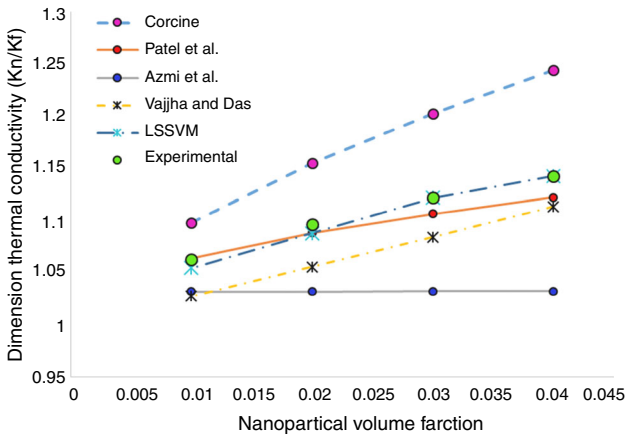

Fig. 11 Comparison of LSSVM model with different models to estimate dimensionless thermal conductivity of CuO–water nanofluid

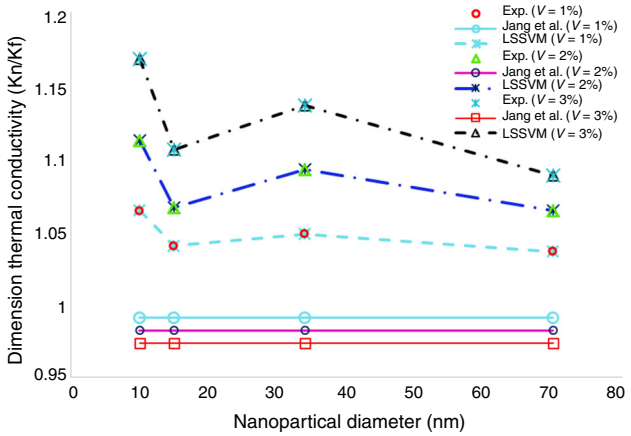

Fig. 12 Comparison of LSSVM model with Jang et al. models to estimate dimensionless thermal conductivity of TiO_2–EG nanofluid for different volume fractions and size particles

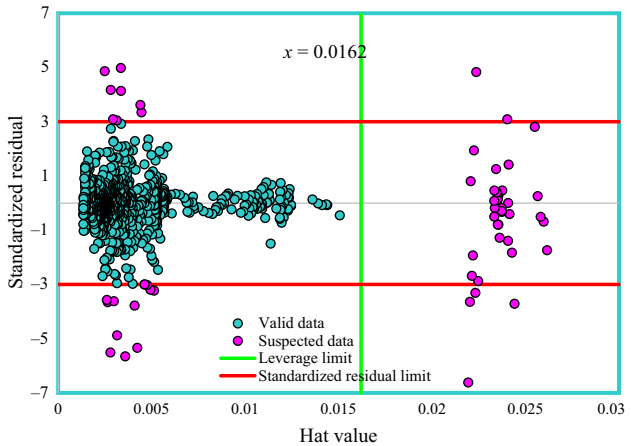

Fig. 13 Outlier analysis of the proposed LSSVM model

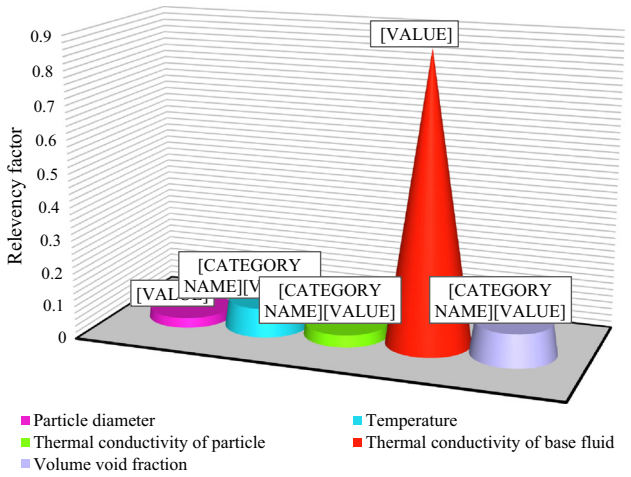

Fig. 14 Sensitivity analysis of parameters used for the developed model

Conclusions

According to the results from statistical analyses and graphical illustrations, we can find significant conclusions as follows:

- A comprehensive databank adopted from previously published articles was used in the present study, and the successful performance of our LSSVM model was shown in order to estimate thermal conductivity of nanofluids.
- Optimizing tuning parameters of LSSVM strategy by PSO algorithm led to encouraging results for predicting thermal conductivity of nanofluids. In addition, a satisfactory agreement was observed between the outcomes of the proposed LSSVM model and experimental values with obtained R^2 and AARD % of 0.9913 and 3.10%, respectively.

Fig. 15 GUI version of developed model for estimation of thermal conductivity of nanofluid

- A comparison of the LSSVM results with 15 different correlations indicates great accuracy. Further, the corresponding predictive capability of our model was greatly accepted. Moreover, we can see a great generalization ability of the LSSVM model to estimate thermal conductivity of different nanofluids.
- The present model is highly nonlinear and complicated. As a result, through using the LSSVM approach, which is a connectionist technique with low tuning parameters, can help to overcome any drawbacks and issues that one might face.

Appendix: Program

I have developed a graphical user interface (GUI) version of the model as illustrated in Fig. 15. This program is an exe file presented in supplementary content, and it needs Matlab software version 2012 (64bit) before running. As indicated, three input parameters (temperature, diameter, and volume fraction) should be given and by choosing one of nanofluid in the panel and then clicking on calculate button, the thermal conductivity of nanofluid is obtained.

References

1. Wen D, Lin G, Vafaei S, Zhang K. Review of nanofluids for heat transfer applications. Particuology. 2009;7:141–50.
2. Zalba B, Marín JM, Cabeza LF, Mehling H. Review on thermal energy storage with phase change: materials, heat transfer analysis and applications. Appl Therm Eng. 2003;23:251–83.
3. Tomlinson HL, Manning W, Schaefer W, Record T (2016) Process for increasing the efficiency of heat removal from a Fischer–Tropsch slurry reactor, Google Patents.
4. Ebrahimnia-Bajestan E, Moghadam MC, Niazmand H, Daungthongsuk W, Wongwises S. Experimental and numerical investigation of nanofluids heat transfer characteristics for application in solar heat exchangers. Int J Heat Mass Transf. 2016;92:1041–52.
5. Mazumdar A, Spencer SJ, Hobart C, Kuehl M, Brunson G, Coleman N, Buerger SP. Improving robotic actuator torque density and efficiency through enhanced heat transfer. In: ASME 2016 Dynamic Systems and Control Conference. American Society of Mechanical Engineers; 2016, p. V002T026A004.
6. Eiamsa-Ard S, Wongcharee K. Experimental study of TiO_2–water nanofluid flow in corrugated tubes mounted with semi-circular wing tapes. Heat Transf Eng. 2018;39:1–14.
7. Zeeshan A, Shehzad N, Ellahi R, Alamri SZ. Convective Poiseuille flow of Al_2O_3–EG nanofluid in a porous wavy channel with thermal radiation. Neural Comput Appl. 2017;28:1–12.
8. Chol S. Enhancing thermal conductivity of fluids with nanoparticles. ASME Publ Fed. 1995;231:99–106.
9. Chein R, Chuang J. Experimental microchannel heat sink performance studies using nanofluids. Int J Therm Sci. 2007;46:57–66.
10. Maxwell JC. A treatise on electricity and magnetism. Oxford: Clarendon Press; 1881.
11. Murshed S, Leong K, Yang C. Investigations of thermal conductivity and viscosity of nanofluids. Int J Therm Sci. 2008;47:560–8.
12. Lee J-H, Lee S-H, Choi C, Jang S, Choi S. A review of thermal conductivity data, mechanisms and models for nanofluids. Int J Micro Nano Scale Transp. 2011;1:269–322.
13. Kleinstreuer C, Feng Y. Experimental and theoretical studies of nanofluid thermal conductivity enhancement: a review. Nanoscale Res Lett. 2011;6:1–13.
14. Keblinski P, Phillpot S, Choi S, Eastman J. Mechanisms of heat flow in suspensions of nano-sized particles (nanofluids). Int J Heat Mass Transf. 2002;45:855–63.
15. Vatani A, Woodfield PL, Dao DV. A survey of practical equations for prediction of effective thermal conductivity of spherical-particle nanofluids. J Mol Liq. 2015;211:712–33.
16. Ariana M, Vaferi B, Karimi G. Prediction of thermal conductivity of alumina water-based nanofluids by artificial neural networks. Powder Technol. 2015;278:1–10.
17. Baghban A, Pourfayaz F, Ahmadi MH, Kasaeian A, Pourkiaei SM, Lorenzini G. Connectionist intelligent model estimates of convective heat transfer coefficient of nanofluids in circular cross-sectional channels. J Therm Anal Calorim. 2017;130:1–27.
18. Baghban A, Ahmadi MA, Shahraki BH. Prediction carbon dioxide solubility in presence of various ionic liquids using computational intelligence approaches. J Supercrit Fluids. 2015;98:50–64.
19. Baghban A, Bahadori A, Mohammadi AH, Behbahaninia A. Prediction of CO_2 loading capacities of aqueous solutions of absorbents using different computational schemes. Int J Greenh Gas Control. 2017;57:143–61.
20. Baghban A, Bahadori M, Rozyn J, Lee M, Abbas A, Bahadori A, Rahimali A. Estimation of air dew point temperature using computational intelligence schemes. Appl Therm Eng. 2016;93:1043–52.
21. Baghban A, Mohammadi AH, Taleghani MS. Rigorous modeling of CO_2 equilibrium absorption in ionic liquids. Int J Greenh Gas Control. 2017;58:19–41.
22. Bahadori A, Baghban A, Bahadori M, Lee M, Ahmad Z, Zare M, Abdollahi E. Computational intelligent strategies to predict energy conservation benefits in excess air controlled gas-fired systems. Appl Therm Eng. 2016;102:432–46.
23. Baghban A, Kardani MN, Habibzadeh S. Prediction viscosity of ionic liquids using a hybrid LSSVM and group contribution method. J Mol Liq. 2017;236:452–64.
24. Karimi H, Yousefi F, Rahimi MR. Correlation of viscosity in nanofluids using genetic algorithm-neural network (GA-NN). Heat Mass Transf. 2011;47:1417–25.
25. Atashrouz S, Pazuki G, Alimoradi Y. Estimation of the viscosity of nine nanofluids using a hybrid GMDH-type neural network system. Fluid Phase Equilib. 2014;372:43–8.
26. Sharifpur M, Adio SA, Meyer JP. Experimental investigation and model development for effective viscosity of Al_2O_3–glycerol nanofluids by using dimensional analysis and GMDH-NN methods. Int Commun Heat Mass Transf. 2015;68:208–19.
27. Karimi H, Yousefi F. Application of artificial neural network–genetic algorithm (ANN–GA) to correlation of density in nanofluids. Fluid Phase Equilib. 2012;336:79–83.
28. Hojjat M, Etemad SG, Bagheri R, Thibault J. Thermal conductivity of non-Newtonian nanofluids: experimental data and modeling using neural network. Int J Heat Mass Transf. 2011;54:1017–23.
29. Papari MM, Yousefi F, Moghadasi J, Karimi H, Campo A. Modeling thermal conductivity augmentation of nanofluids using diffusion neural networks. Int J Therm Sci. 2011;50:44–52.

30. Longo GA, Zilio C, Ceseracciu E, Reggiani M. Application of artificial neural network (ANN) for the prediction of thermal conductivity of oxide–water nanofluids. Nano Energy. 2012;1:290–6.
31. Esfe MH, Afrand M, Yan W-M, Akbari M. Applicability of artificial neural network and nonlinear regression to predict thermal conductivity modeling of Al_2O_3–water nanofluids using experimental data. Int Commun Heat Mass Transf. 2015;66:246–9.
32. Meybodi MK, Naseri S, Shokrollahi A, Daryasafar A. Prediction of viscosity of water-based Al_2O_3, TiO_2, SiO_2, and CuO nanofluids using a reliable approach. Chemom Intell Lab Syst. 2015;149:60–9.
33. Maxwell J. Electricity and magnetism. Oxford: Clarendon Press; 1873.
34. Hamilton R, Crosser O. Thermal conductivity of heterogeneous two-component systems. Ind Eng Chem Fundam. 1962;1:187–91.
35. Bruggeman VD. Berechnung verschiedener physikalischer Konstanten von heterogenen Substanzen. I. Dielektrizitätskonstanten und Leitfähigkeiten der Mischkörper aus isotropen Substanzen. Ann Phys. 1935;416:636–64.
36. Yu W, Choi S. The role of interfacial layers in the enhanced thermal conductivity of nanofluids: a renovated Maxwell model. J Nanopart Res. 2003;5:167–71.
37. Leong K, Yang C, Murshed S. A model for the thermal conductivity of nanofluids—the effect of interfacial layer. J Nanopart Res. 2006;8:245–54.
38. Xie H, Fujii M, Zhang X. Effect of interfacial nanolayer on the effective thermal conductivity of nanoparticle-fluid mixture. Int J Heat Mass Transf. 2005;48:2926–32.
39. Sohrabi N, Masoumi N, Behzadmehr A, Sarvari S. A simple analytical model for calculating the effective thermal conductivity of nanofluids. Heat Transf Asian Res. 2010;39:141–50.
40. Koo J, Kleinstreuer C. A new thermal conductivity model for nanofluids. J Nanopart Res. 2004;6:577–88.
41. Xu J, Yu B, Zou M, Xu P. A new model for heat conduction of nanofluids based on fractal distributions of nanoparticles. J Phys D Appl Phys. 2006;39:4486.
42. Evans W, Prasher R, Fish J, Meakin P, Phelan P, Keblinski P. Effect of aggregation and interfacial thermal resistance on thermal conductivity of nanocomposites and colloidal nanofluids. Int J Heat Mass Transf. 2008;51:1431–8.
43. Schwartz LM, Garboczi EJ, Bentz DP. Interfacial transport in porous media: application to DC electrical conductivity of mortars. J Appl Phys. 1995;78:5898–908.
44. Tomotika S, Aoi T, Yosinobu H. On the forces acting on a circular cylinder set obliquely in a uniform stream at low values of Reynolds number. In: Proceedings of the Royal Society of London A: Mathematical, Physical and Engineering Sciences, The Royal Society; 1953, p. 233–244.
45. Prasher R, Phelan PE, Bhattacharya P. Effect of aggregation kinetics on the thermal conductivity of nanoscale colloidal solutions (nanofluid). Nano Lett. 2006;6:1529–34.
46. He Y, Jin Y, Chen H, Ding Y, Cang D, Lu H. Heat transfer and flow behaviour of aqueous suspensions of TiO_2 nanoparticles (nanofluids) flowing upward through a vertical pipe. Int J Heat Mass Transf. 2007;50:2272–81.
47. Wang B-X, Zhou L-P, Peng X-F. A fractal model for predicting the effective thermal conductivity of liquid with suspension of nanoparticles. Int J Heat Mass Transf. 2003;46:2665–72.
48. Nan C-W, Birringer R, Clarke DR, Gleiter H. Effective thermal conductivity of particulate composites with interfacial thermal resistance. J Appl Phys. 1997;81:6692–9.
49. Suykens JA, Vandewalle J. Least squares support vector machine classifiers. Neural Process Lett. 1999;9:293–300.
50. Suykens JA, Vandewalle J. Recurrent least squares support vector machines. IEEE Trans Circuits Syst I Fundam Theory Appl. 2000;47:1109–14.
51. Suykens JA, Van Gestel T, De Brabanter J. Least squares support vector machines. Singapore: World Scientific; 2002.
52. Guo Z, Bai G. Application of least squares support vector machine for regression to reliability analysis. Chin J Aeronaut. 2009;22:160–6.
53. Nan C-W, Shi Z, Lin Y. A simple model for thermal conductivity of carbon nanotube-based composites. Chem Phys Lett. 2003;375:666–9.
54. Rashmi W, Khalid M, Ismail AF, Saidur R, Rashid A. Experimental and numerical investigation of heat transfer in CNT nanofluids. J Exp Nanosci. 2015;10:545–63.
55. Jiang H, Li H, Zan C, Wang F, Yang Q, Shi L. Temperature dependence of the stability and thermal conductivity of an oil-based nanofluid. Thermochim Acta. 2014;579:27–30.
56. Kazemi-Beydokhti A, Heris SZ, Moghadam N, Shariati-Niasar M, Hamidi A. Experimental investigation of parameters affecting nanofluid effective thermal conductivity. Chem Eng Commun. 2014;201:593–611.
57. Murshed SS. Simultaneous measurement of thermal conductivity, thermal diffusivity, and specific heat of nanofluids. Heat Transf Eng. 2012;33:722–31.
58. Patel HE, Sundararajan T, Das SK. An experimental investigation into the thermal conductivity enhancement in oxide and metallic nanofluids. J Nanopart Res. 2010;12:1015–31.
59. Chon CH, Kihm KD, Lee SP, Choi SU. Empirical correlation finding the role of temperature and particle size for nanofluid (Al_2O_3) thermal conductivity enhancement. Appl Phys Lett. 2005;87:153107.
60. Mintsa HA, Roy G, Nguyen CT, Doucet D. New temperature dependent thermal conductivity data for water-based nanofluids. Int J Therm Sci. 2009;48:363–71.
61. Godson L, Raja B, Lal DM, Wongwises S. Experimental investigation on the thermal conductivity and viscosity of silver-deionized water nanofluid. Exp Heat Transf. 2010;23:317–32.
62. Thang BH, Khoi PH, Minh PN. A modified model for thermal conductivity of carbon nanotube-nanofluids. Phys Fluids. 2015;27:032002.
63. Das SK, Putra N, Thiesen P, Roetzel W. Temperature dependence of thermal conductivity enhancement for nanofluids. J Heat Transf. 2003;125:567–74.
64. Lee S, Choi S-S, Li S, Eastman J. Measuring thermal conductivity of fluids containing oxide nanoparticles. J Heat Transf. 1999;121:280–9.
65. Kim SH, Choi SR, Kim D. Thermal conductivity of metal-oxide nanofluids: particle size dependence and effect of laser irradiation. J Heat Transf. 2007;129:298–307.
66. Khedkar RS, Sonawane SS, Wasewar KL. Influence of CuO nanoparticles in enhancing the thermal conductivity of water and monoethylene glycol based nanofluids. Int Commun Heat Mass Transf. 2012;39:665–9.
67. Zerradi H, Ouaskit S, Dezairi A, Loulijat H, Mizani S. New Nusselt number correlations to predict the thermal conductivity of nanofluids. Adv Powder Technol. 2014;25:1124–31.
68. Eastman JA, Choi S, Li S, Yu W, Thompson L. Anomalously increased effective thermal conductivities of ethylene glycol-based nanofluids containing copper nanoparticles. Appl Phys Lett. 2001;78:718–20.
69. Moghadassi A, Hosseini SM, Henneke DE. Effect of CuO nanoparticles in enhancing the thermal conductivities of monoethylene glycol and paraffin fluids. Ind Eng Chem Res. 2010;49:1900–4.

70. Fedele L, Colla L, Bobbo S. Viscosity and thermal conductivity measurements of water-based nanofluids containing titanium oxide nanoparticles. Int J Refrig. 2012;35:1359–66.
71. Pastoriza-Gallego M, Lugo L, Cabaleiro D, Legido J, Piñeiro M. Thermophysical profile of ethylene glycol-based ZnO nanofluids. J Chem Thermodyn. 2014;73:23–30.
72. Mondragón R, Segarra C, Martínez-Cuenca R, Juliá JE, Jarque JC. Experimental characterization and modeling of thermophysical properties of nanofluids at high temperature conditions for heat transfer applications. Powder Technol. 2013;249:516–29.
73. Halelfadl S, Maré T, Estellé P. Efficiency of carbon nanotubes water based nanofluids as coolants. Exp Therm Fluid Sci. 2014;53:104–10.
74. Chen L, Xie H, Li Y, Yu W. Nanofluids containing carbon nanotubes treated by mechanochemical reaction. Thermochim Acta. 2008;477:21–4.
75. Hwang Y, Ahn Y, Shin H, Lee C, Kim G, Park H, Lee J. Investigation on characteristics of thermal conductivity enhancement of nanofluids. Curr Appl Phys. 2006;6:1068–71.
76. Jiang W, Ding G, Peng H. Measurement and model on thermal conductivities of carbon nanotube nanorefrigerants. Int J Therm Sci. 2009;48:1108–15.
77. Choi S, Zhang Z, Yu W, Lockwood F, Grulke E. Anomalous thermal conductivity enhancement in nanotube suspensions. Appl Phys Lett. 2001;79:2252–4.
78. Godson L, Lal DM, Wongwises S. Measurement of thermo physical properties of metallic nanofluids for high temperature applications. Nanoscale Microscale Thermophys Eng. 2010;14:152–73.
79. Timofeeva EV, Moravek MR, Singh D. Improving the heat transfer efficiency of synthetic oil with silica nanoparticles. J Colloid Interface Sci. 2011;364:71–9.
80. Wasp EJ, Kenny JP, Gandhi RL. Solid–liquid flow: slurry pipeline transportation. [Pumps, valves, mechanical equipment, economics]. Ser Bulk Mater Handl U S 1977;1.
81. Corcione M. Empirical correlating equations for predicting the effective thermal conductivity and dynamic viscosity of nanofluids. Energy Convers Manag. 2011;52:789–93.
82. Azmi W, Sharma K, Mamat R, Alias A, Misnon II. Correlations for thermal conductivity and viscosity of water based nanofluids. In: IOP Conference Series: Materials Science and Engineering. IOP Publishing; 2012, p. 012029.
83. Vajjha RS, Das DK. Experimental determination of thermal conductivity of three nanofluids and development of new correlations. Int J Heat Mass Transf. 2009;52:4675–82.
84. Jang SP, Choi SU. Role of Brownian motion in the enhanced thermal conductivity of nanofluids. Appl Phys Lett. 2004;84:4316–8.
85. Rousseeuw PJ, Leroy AM. Robust regression and outlier detection. New York: Wiley; 2005.
86. Mohammadi AH, Gharagheizi F, Eslamimanesh A, Richon D. Evaluation of experimental data for wax and diamondoids solubility in gaseous systems. Chem Eng Sci. 2012;81:1–7.
87. Hosseinzadeh M, Hemmati-Sarapardeh A. Toward a predictive model for estimating viscosity of ternary mixtures containing ionic liquids. J Mol Liq. 2014;200:340–8.